Foaming and cross-linking of cellulose fibers using phytic acid

Carbohydrate Polymers 347 (2025) 122617

Contents lists available at ScienceDirect

Carbohydrate Polymers

journal homepage: www.elsevier.com/locate/carbpol

Foaming and cross-linking of cellulose fibers using phytic acid

E. Orzan [a], A. Barrio [b], V. Biegler [c], J.B. Schaubeder [d], A. Bismarck [c], S. Spirk [d], T. Nypelö [a,e,*]

[a] Department of Chemistry and Chemical Engineering, Chalmers University of Technology, Kemivägen 10, Gothenburg 41296, Sweden
[b] TECNALIA, Basque Research and Technology Alliance (BRTA), Area Anardi 5, Azpeitia 20730, Spain
[c] Institute for Materials Chemistry and Research, University of Vienna, Währinger Straße 42, Vienna 1090, Austria
[d] Institute of Bioproducts and Paper Technology, Graz University of Technology, Inffeldgasse 23, Graz 8010, Austria
[e] Department of Bioproducts and Biosystems, Aalto University, Vuorimiehentie 1, Aalto FI-00076, Finland

ARTICLE INFO

Keywords:
Phosphate
Flame retardant
Cellular solid
Biopolymer
Frothing
Porous network

ABSTRACT

Bio-based compounds have become the focus in the development of next-generation materials. The polyphosphated structure and availability of phytic acid has sparked an interest to understand its properties and apply it to making fire-retardant fabrics. However, its degradative effect on natural fibers sets limitations to its potential uses. In this study, we unveiled a new dimension to explore with phytic acid: cellulose fiber foams. Phytic acid enabled synergistic foaming with carboxymethyl cellulose albeit causing issues in long-term wet foam stability. Adding cellulose fibers to this mixture and drying at 160 °C produced solid foams with increased compressive strength and stiffness; comparable to foams cross-linked with the commonly used citric acid. The reduced contact area in low-density fiber networks allowed the cross-linking between phytic acid and the fiber network to mitigate structural weakening due to fiber degradation. Imaging also revealed the formation of a film encompassing fiber bonds; attributed to the strong interaction between phytic acid and carboxymethyl cellulose. Furthermore, phytic acid imparted self-extinguishing fire-retardant properties to the cellulose fiber foams measured using thermogravimetric analysis and cone calorimetry. This work showcases a simple new application for phytic acid without the use of catalysts or solvents. It serves to encourage further development of green practices to continuously challenge the industrial landscape.

1. Introduction

Cellulose fiber foams are prominent industrial solutions for bio-based packaging and insulation applications. However, these solid foams have yet to breach into the construction and transportation sectors, which demand competitive compressive strength and stiffness. For such applications the dominance of petroleum-based foams has yet to be challenged. One of the limitations of cellulose-based foams is their poor compressive modulus and strength, leading to performance issues under high compressive load and requiring the use of additives to be more competitive (Ferreira, Rezende, & Cranston, 2021). Efforts to strengthen cellulose fiber foams have turned to citric acid (CA) as a cross-linking agent. Reacting CA at temperatures above 160 °C creates covalent ester bonds to cellulose and acts as a bridge between fibers (Yang, Wang, & Kang, 1997). These bonds strengthen fiber-fiber contacts and thus enable the fiber network to act cohesively under load instead of as individual fibers (Ketoja, Paunonen, Jetsu, & Pääkkönen, 2019; Pöhler et al., 2020). Besides improved strength, such foams would also benefit from flame-retardancy to remain relevant for commercial use. However, CA has shown little to no relevant fire-retardant properties (Hassan, Tucker, & Le Guen, 2020).

Phytic acid (PA), (1R,2S,3r,4R,5S,6s)-cyclohexane-1,2,3,4,5,6-hexayl hexakis[dihydrogen (phosphate)] or inositol hexakisphosphate, is a polyphosphate derived from the plant tissues of seeds, legumes and bran. Its discovery in the 1970s led to a surge of research vying to understand its sources, derivatives and properties. As a food component, it acts as an anti-nutrient by chelating metal ions to its acidic phosphate groups. This led to the use of PA as an anti-bacterial agent and conductivity promoter in, for example, wearable sensors on skin (Du et al., 2022; Ghilan et al., 2022; Hou et al., 2022; Jiang, Qiao, & Hong, 2012; Li, Sun, He, Liu, & Wang, 2023). The six-fold presence of phosphates is of particular interest to this work, as phosphorus has defined the large-scale transition toward non-toxic, bio-based options for flame-retardant materials.

Phytic acid has become a prime candidate in the creation of high performance fire-retardant cellulose-based fabrics made from cotton

* Corresponding author at: Department of Chemistry and Chemical Engineering, Chalmers University of Technology, Kemivägen 10, Gothenburg 41296, Sweden.
E-mail address: tiina.nypelo@aalto.fi (T. Nypelö).

https://doi.org/10.1016/j.carbpol.2024.122617
Received 5 April 2024; Received in revised form 9 August 2024; Accepted 14 August 2024
Available online 22 August 2024

and wool (Barbalini, Bertolla, Toušek, & Malucelli, 2019; Cheng, Wang, Jin, & Guan, 2022; Du et al., 2022; Feng et al., 2017; Hou et al., 2022; Liu et al., 2018; Liu et al., 2022; Ma et al., 2021; Song et al., 2022; Sun et al., 2021; Thota et al., 2020; Zheng, Dong, Liu, Xu, & Jian, 2022). We recently showed a catalyst- and solvent-less methodology to form covalent ester bonds between cellulose and PA through NMR, FTIR, XPS and elemental analysis by drying a cellulose substrate at 160 °C. (Orzan, Barrio, Spirk, & Nypelö, 2024) However, studies have reported a decrease in tensile properties on account of the cellulose fiber degradation caused by phytic acid hydrolysis (Antoun et al., 2022; Feng et al., 2017; Jiang et al., 2012; Liu et al., 2022; Ma et al., 2021; Song et al., 2022; Sun et al., 2021; Thota et al., 2020). The use of cross-linking agents such as urea and dicyandiamide has mitigated some damage and discoloration, yet many still reported decreased tensile properties. Here, we aim to verify whether these observations hold true for cellulose fiber foams cross-linked with PA, subjected to compressive load. Two separate studies performed compression testing of solid foams using cellulose and PA, with both revealing an increase in modulus (stiffness) and strength. (Ding, Qiu, Wang, Song, & Hu, 2021; Ren et al., 2022). However, the 2–3 fold increase in density resulting from the addition of large quantities of phytic acid was not accounted for, although the densification of pore cell walls is known to improve gel/foam strength by increasing fiber-fiber contacts (Ganesan, Barowski, Ratke, & Milow, 2019; Gibson, 2003; Ketoja et al., 2019). Thus, the effect of phytic acid cross-linking on a cellulose fiber network has thus far remained unelucidated.

Studies creating porous gels comprising PA have formed self-standing stable gels by relying on attractive electrostatic interactions using carboxymethyl cellulose (CMC) (Ghilan et al., 2022), guanazole (Ding et al., 2021), melamine (Ren et al., 2022), or metal cations (Cai et al., 2019; Gao et al., 2022; Xiao, Gong, & Zhang, 2021). These gels were dried into solid foams using supercritical CO_2 or freeze-drying, two common methods to generate porosity. However, using a frothing technique (mechanical agitation) with ionic surfactants to foam cellulose fibers and PA has not yet been explored. When creating a frothed foam, foaming agents such as surfactants trap gasses within a liquid media by decreasing surface tension and stabilizing the interfaces between bubbles. As attractive van der Waal forces bring bubbles closer together, drainage of the liquid between the membranes threatens to rupture the interfaces. The rupture causes bubble coalescence and release of the trapped gasses, ultimately leading to the collapse of the foam. To stabilize wet foams, the repulsive electrostatic forces generated by sodium dodecyl sulfate (SDS), an ionic surfactant with negatively charged sulfate groups, create an equilibrium and stabilize the interfaces (Bikerman, 1973; Evans & Wennerström, 1999; Guerrini, Lochhead, & Daly, 1999).

A wet foam may also be stabilized through the incorporation of polymers, which physically encapsulate gas bubbles and increase viscosity of the continuous phase (Evans & Wennerström, 1999). CMC was thus incorporated to act as a secondary stabilizing agent, while also improving the homogeneity of fibers during mixing and strengthening fiber-fiber bonding (Pöhler et al., 2020). The foaming/frothing process heavily relies on the interactions between CMC, SDS, acids (PA or CA) and cellulose fibers. To evaluate foaming behaviour, three parameters were investigated: foamability, maximum foam height, and foam stability. Foamability represents the amount of mixing time (t_{max}) necessary to reach a maximum foam height (H_{max}). At maximum foam height, a steady state between foam forming (bubble production) and collapsing (drainage and coalescence) is established. The foam stability is then determined as the rate at which the wet foam collapses.

We aim to showcase the potential of phytic acid in i) the creation of and ii) strengthening and flame-retardancy of cellulose foams. In the formation of wet foams, we hypothesize that phytic acid molecules interact favourably with CMC and SDS to electrostatically stabilize air bubbles in liquid media credit to the six negatively charged phosphate groups that lead to repulsion and a foam stabilizing effect. Drying the wet foams at 160 °C then creates strong cross-links between PA and cellulose fibers, akin to CA cross-linking. In the dry foams, tuning drying temperature and using a low concentration of phytic acid prevents severe cellulose degradation while binding the fiber network to improve compressive strength. Cone calorimeter analysis demonstrates how phytic acid induces fire-retardancy in cellulose-fiber foams, complying to green chemistry principles.

2. Experimental

2.1. Materials

Dried, bleached kraft wood pulp (hardwood; 100 % birch and softwood; 85 % spruce, 10 % pine, 5 % larch) were kindly provided by Stora Enso (Sweden) and Heinzel Pulp Zellstoff Pöls (Austria), respectively. Monosaccharide analysis was performed following acid hydrolysis (Theander & Westerlund, 1986) and revealed the pulps to consist of 73 % cellulose, 26 % hemicelluloses for hardwood and 83 % cellulose, 16 % hemicelluloses for softwood. Klason and acid soluble lignins were analyzed via gravimetric and UV spectroscopy methods respectively, finding a lignin content of 1 % in both pulps.

Sodium CMC (molar mass ~ 250,000 g/mol, degree of substitution 0.7), phytic acid solution (50 % *w*/w in H_2O), citric acid powder, and SDS powder were purchased from Merck (Sweden). All reagents purchased were used without further purification.

2.2. Wet foam analysis

Foaming was performed using an IKA EUROSTAR 60 overhead stirrer equipped with the R-1342 4-bladed propeller stirrer. Solutions with combinations of 0.1 wt% SDS, 0.6 wt% CMC, and 0.6 wt% phytic acid (PA) or citric acid (CA) were filled to 100 mL with deionized (DI) water in a narrow beaker. The chosen concentrations were the same as those used in the creation of the cellulose-fiber foams. Wood pulp fibers were not included in the wet foam composition, as the drastic increase in viscosity caused large displacements within the measuring device, making proper analysis difficult. After 5 min of stirring at 200 rpm, stirring was stopped and started again at 1500 rpm for 20 min to achieve maximum foam height. Height increase during foaming was recorded using a GoPro Hero 8 Black video camera and measured with a fixed ruler. A correlation between beaker volume and ruler height was established beforehand to determine the approximate volume to the nearest 3 mL.

Analysis on foamability, maximum foam height and foam stability was used to understand interactions between phytic acid and other additives in the production of wet foams (air trapped in liquid media). Foamability is defined as the rate at which volume increases until reaching the maximum foam height (H_{max}). The foaming is then stopped to measure foam stability (volume collapse) over time.

2.3. Cellulose foam preparation

Softwood pulp sheets were dispersed in distilled water with a Noram disintegrator to 4 wt% consistency and then drained to 14 wt%. Hardwood pulp sheets were soaked overnight in distilled water and refined for 15 min (to 25°SR) in a valley beater according to ISO 5264-1. The refined pulp suspension was reduced to a consistency of 14 wt%. Additives were dissolved in distilled water to consistencies of: 5 wt% (CMC, 2 mmol/L), 5 wt% (SDS, 1.8 mm/L), 50 wt% (phytic acid, 7.5 mmol/L). Softwood (70.7 g of 14 wt%) and hardwood (23.6 g of 14 wt%) pulps were mixed together using a hand-held mixer (Bosch MFQ3030 CleverMixx 350 W) at speed setting 1 with either PA, CA, or no acid (1.134 mL of 50 wt% acid) until homogeneous. A 3:1 ratio of non-fibrillated softwood to 25° SR fibrillated hardwood pulp was chosen to create an interconnected matrix. The CMC (14.5 g of 5 wt%) and SDS (2 mL of 5 wt %) were added to the wet formulation and mixed at speed 3 for about 30

s to create a wet foam. The wet foam was transferred into a 10 × 10 × 2 cm Teflon mold and dried at 80 °C in a convection oven for 12 h to a constant moisture content of 5 wt%. Dried foams were then reacted at 80, 120 and 160 °C for 180, 120, and 5 min respectively to replicate conditions used for cellulosic materials.(Demitri et al., 2008; Ferreira, Cranston, & Rezende, 2020; Frone et al., 2020; Meftahi, Khajavi, Rashidi, Rahimi, & Bahador, 2018; Orzan et al., 2024; Štiglic et al., 2022; Yang et al., 1997). Samples were labeled starting with the letter of the acid used (e.g. P for phytic acid, C for citric acid) and then the reaction temperature used after drying.

2.4. Density and porosity

Solid foams were all prepared in order to reach a density of 75 kg/m^3. To account for discrepancies in density due to shrinkage, relative density was determined. Relative density, ρ_R, is given as the ratio of the envelope density to skeletal density (Eq. (1)) (Gibson, 2003). Solid foams were cut into 3 × 3 × 2 cm cubes using a bandsaw. The envelope density (ρ_E) was measured using calipers and a high-precision balance. Skeletal density (ρ_S) was measured using He gas in a Micromeritics AccuPyc II gas displacement pycnometer. Porosity was then calculated using Eq. (2) (Gibson, 2003).

$$\rho_R = \frac{\rho_E}{\rho_S} \tag{1}$$

$$\text{Porosity } (\%) = (1 - \rho_R)\cdot 100 \tag{2}$$

2.5. Moisture absorption

Moisture absorption of 10 × 10 × 2 cm foam panels was performed in an empty desiccator containing a large beaker of a saturated NaCl solution to create a 75 % relative humidity (RH) environment. Prior to measurement, the foams were placed directly inside a separate desiccator containing silica gel beads after drying to remove any residual moisture. The panels were measured gravimetrically at regular intervals to evaluate the percent uptake of water by weight.

2.6. Scanning Electron Microscopy (SEM)

The cellulose fiber foams were cut using a thin blade through the center and the top surface layer. The foams were put in a dessicator for 1 day before sputter-coated with 4 nm of gold and visualized on a JEOL 7800F Prime at an acceleration voltage of 5 kV.

2.7. Mechanical compression

Quasi-static mechanical compression testing was performed in an Instron 5565 A Universal Testing Machine to evaluate the performance of the solid foams. 3 × 3 × 2 cm cellulose fiber foam cubes were evaluated using 4 cubes from triplicate foam batches (10–12 tests for each foam type). The pre-cut cubes were conditioned at 20 °C in a desiccator for a week before testing. A 5 kN load cell applied a compression rate of 5 mm/min after reaching a pre-load force of 5 N to account for any irregularities in the morphology of the foams. The test was ended after densification was achieved around 70 % strain. Raw data was recorded using the Instron BlueHill 2 software. A script was devised in MathWorks MATLAB to calculate modulus, strength and energy absorption. Compressive modulus was taken as the slope of the stress-strain curve below 10 % strain, while the compressive strength corresponded to the stress at 10 % strain. Energy absorption was calculated as the area under the stress-strain curve up to 50 % strain. All calculated values were divided by their respective relative densities.

2.8. Thermogravimetric analysis (TGA)

To understand the thermo-oxidative degradation behaviour of cross-linked cellulose fiber foams when exposed to heat, TGA analysis was used. A Mettler Toledo TGA/DSC 3+ was utilized under the following heating sequence managed by STARe Software: 1. Ramp from 30 °C – 500 °C at a rate of 10 K/min under 60 mL/min air flow, 2. Temperature hold at 500 °C for 5 min, 3. Ramp from 500 °C – 700 °C at a rate of 10 K/min under 60 mL/min air flow, 4. Temperature hold at 800 °C for 10 min. The reported values are an average of 3 substrates taken from separate batches. Carbonization onset was set as the point where the slope of the graph deviated by more than 3 %. Weight loss and the rate of carbonization were calculated from this point to where the slope begins levelling out as indicated by a change in slope of 30 %. Degradation rate was taken as the slope from the start of the plateau to the final drop in weight. Finally, residual weight was taken as the weight percent of the material at 700 °C.

2.9. Cone calorimetry

A medium thermal attack was applied with a flux of 35 kW/m^2 (ISO 5660-3). The separation of the sample from the resistance coil was 25 mm and the test time was 700 s. All the tests were done in triplicates. Analysis was performed on the following key parameters: Time to Ignition (TTI: s), Peak Heat Release Rate (PHRR: kW/m^2), Time to PHRR (TP: s), Fire Growth Rate (FGR: kJ/m^2/s), Total Heat Release (THR: MJ/m^2), Total Smoke Production (TSP: m^2) and Smoke Production Rate (m^2/s).

2.10. Statistical analysis

Statistical analysis was used to determine differences between groups of samples using the Microsoft Excel Data Analysis toolpack. The ANOVA tool (analysis of variance) with $\alpha = 0.05$ was applied to determine whether different temperatures and additives were statistically different. *t*-tests were then conducted to confirm differences between individual groups. Quasi-static compression, TGA and cone calorimetry samples were all performed with triplicate batches.

3. Results and discussion

3.1. Foaming of phytic acid solutions

Negligible differences in maximum foam height (H_{max}) and foamability were observed when frothing a solution of SDS versus one with added phytic acid (PA) (Fig. 1a and Table 1). The trend of foam volume rise over time was similar yet shifted to the right, indicating that PA delayed the rise to H_{max} (Supporting Information Fig. S1a). The post-foaming destabilization of the wet foam was three times faster with PA present (Fig. 1b). The addition of PA dropped the pH in solution from 6.4 to 1.6, where both SDS and PA became protonated (pKa ≈ 3.3 for SDS and 1.6 for PA) (Moosavi-Movahedi et al., 2005). This suggests that bubble stabilization via electrostatic repulsion decreased, which reduced the energy barrier toward coalescence. Thus, the bubbles in the wet foam containing PA collapsed faster, causing the delay to H_{max} and decreasing foam stability post-foaming. Liquid drainage from the lamellae between bubbles was similar for both solutions (Supporting Information Fig. S1b). The setup and maximum foam volume for the solution of SDS and PA can be seen in Figs. 1i,ii. Foaming a solution consisting of PA and CMC generated more air bubbles compared to CMC by itself (Figures 1iii,iv). Here, the drop in pH to 2.0 left CMC protonated while the PA phosphates were deprotonated, unlike the solution of SDS and PA (pka ≈ 4.5 for CMC (Zhivkov, 2013)). The deprotonated PA molecules likely generated electrostatic repulsive forces between bubbles and hydrogen bonded to CMC, creating a stabilized foam (Ghilan et al., 2022).

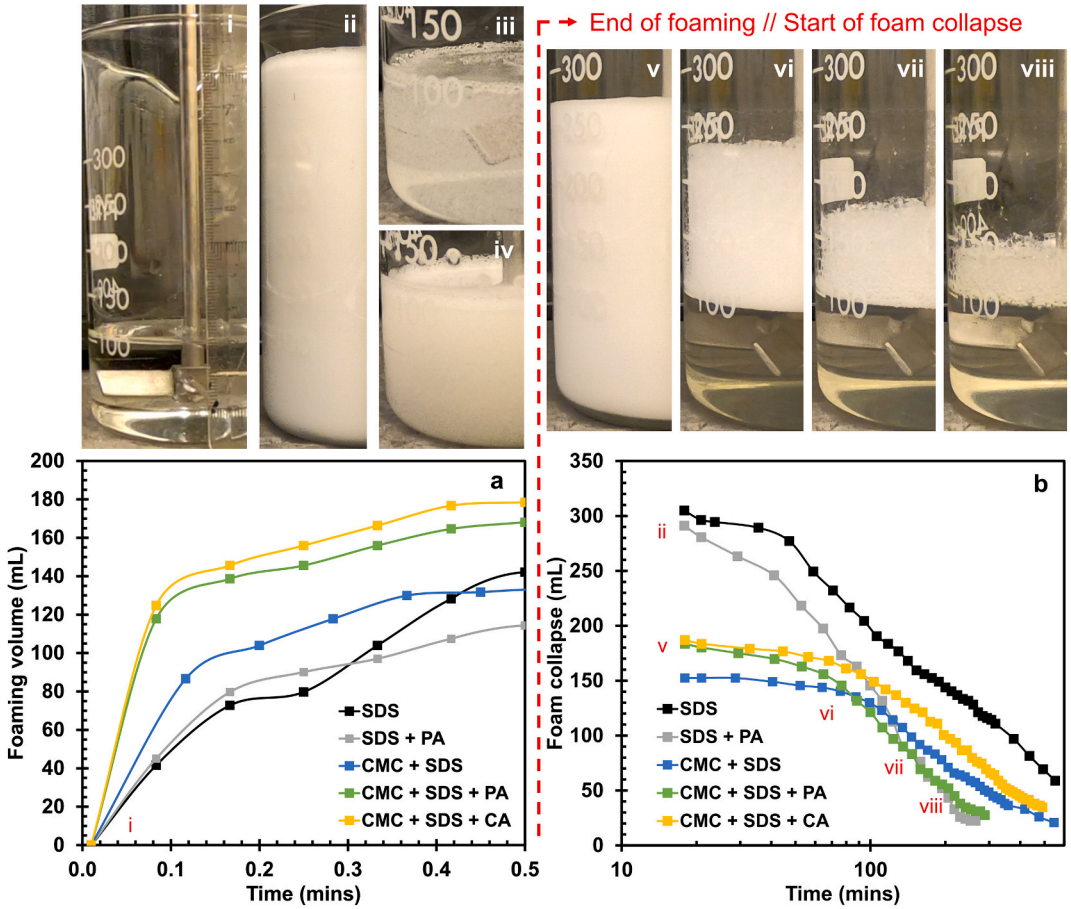

Fig. 1. Wet foam analysis of additive combinations containing 0.1 wt% SDS, 0.6 wt% CMC, 0.6 wt% phytic acid (PA) and 0.6 wt% citric acid (CA) in water. The volumetric change in the foams is shown during a) foaming on a time scale from 0 to 30 s (i = setup at 0 min, ii = SDS + PA at 18 min, iii = CMC at 18 min, iv = CMC + PA at 18 min) and b) foam collapse starting at 18 min (v - viii = CMC + SDS + PA at 18 min, 1 h, 2 h, 3 h, respectively). Lines are provided to guide the eye in observing trends.

Table 1
Wet foam analysis when mixing additive combinations of 0.1 wt% SDS, 0.6 wt% CMC, 0.6 wt% phytic acid (PA) and 0.6 wt% citric acid (CA) in water. t_{max} represents the time to reach maximum foam height, H_{max}. Foamability describes the volume of foam generation within the first 30 s as a rate. t_{20} describes the time to reach 20 % of maximum foam height after foaming is stopped while the foam stability is the linear rate at which the foam volume decreases.

Foam additives[a]	t_{max} (s)	H_{max} (mL)	Foamability (mL/min)	t_{20} (min)	Stability (mL/min)	pH
SDS	360	308	310	523	−0.47	6.4
SDS + PA	420	298	290	150	−1.55	1.6
CMC + SDS	300[b]	152	350	419	−0.29	7.1
CMC + SDS + PA	180[b]	184	470	216	−0.68	2.0
CMC + SDS + CA	30[b]	187	500	443	−0.34	3.2

[a] Phytic acid by itself showed no foaming behaviour and thus is not included.
[b] Foaming continues past noted time at slow rate (true $t_{max} \geq 30$ min), t_{max} is calculated at 95 % of true H_{max} to be representative.

The combination of PA, CMC and SDS formed wet foams with the highest foamability and stability. The addition of acids to CMC and SDS, whether PA or CA, improved both H_{max} and foamability by over 20 % and 35 % respectively. Hydrogen bonding between CMC and PA created physically encapsulated bubbles which were prevented from coalescing via the reduction in surface tension brought by SDS. However, the acids again caused a decrease in foam stability. When adding PA, the pH of the solution dropped from 7.1 to 2.0, causing the protonation of SDS and CMC. The repulsive electrostatic forces which kept bubbles from coalescing during drainage are likely reduced, leading to faster foam collapse (Figs. 1v-viii).

Wet foams comprising CA, CMC and SDS generated negligible improvements to foamability and foam height compared to PA wet foams (6 % and 3 %, respectively). While the drainage rate was unaffected, the stability of CA wet foams was higher, similar to that of the CMC and SDS solution (Fig. 1b and Table 1). CA is a weak acid, and thus only lowered the pH value to 3.2 when adding a similar (*w/w*) amount as PA to the CMC and SDS solution. With the pKa of CA standing at 3.13, the system contained protonated SDS and CMC molecules and deprotonated acid molecules, similarly to the PA wet foam. However, the smaller molecular weight of CA incorporates more acid molecules in solution, which suggests that the 3–4 fold increase of negatively charged CA molecules are critical toward the improved foam stability of bubbles over PA.

3.2. Compression and morphology of solid foams

Dividing the material properties by their relative densities accounted for differences in the porosities of the solid foams (95 ± 0.3 %). Upon addition of PA, a balance is struck between cellulose fiber degradation due to exposure to PA and cross-linking credit to the formation of covalent bonds. The degradation (hydrolysis) removes some of the amorphous bulk surrounding each fiber, decreasing potential fiber-fiber contact area and therefore compromising the network strength. However, at temperatures above 160 °C, cellulose fibers form covalent bonds to PA via condensation reactions, which can drastically increase contact

strength via cross-linking.

The effect of reaction temperature on the compressive properties of solid foams without added acids was determined to be statistically insignificant (Fig. 2 and Supporting Information Table S1). The effect of PA degradation on the fiber network is clear when comparing the properties of the cellulose fiber foams reacted with PA at 80 °C (P80) to the blank foam without acids (80). Stiffness, strength and toughness simultaneously decreased due to the addition of PA (Fig. 2). Therefore, degradation becomes the dominant regime toward compressive behaviour as the removed non-crystalline regions no longer play a supporting structural role in the fiber network.

Increasing the reaction temperature to 120 °C brings the compressive properties of cellulose fiber foams with PA (P120) to equivalence with the blank foams (120) (Fig. 2). Foams cross-linked with PA at a temperature of 160 °C (P160) produced an increase of 60 % in modulus and 15 % in strength compared to blank foams (Fig. 2 and Supporting Information Table S1). The cross-linking achieved at 160 °C subjugated any detriment to the structural strength of the fiber network caused by PA degradation. Comparison with cellulose fiber foams reacted with CA at a similar temperature shows that PA can produce higher stiffness at < 10 % strain (Fig. 2a). However, energy absorption of the fiber foams reacted at 160 °C with CA improved by nearly 20 % over PA solid foams (Fig. 2b).

A common practice to coat fabrics is to immerse cellulosic materials in a concentrated bath of PA for a period of time before drying to ensure high inclusion levels of PA (Barbalini et al., 2019; Cheng et al., 2022; Feng et al., 2017; Ghanadpour, Carosio, Larsson, & Wågberg, 2015; Jiang et al., 2012; Ma et al., 2021; Sun et al., 2021). In comparison to the large amount of publications depicting a decrease in tensile properties for fabrics reacted with PA, here we present how low-density fiber networks can overcome the reduced mechanical properties from fiber hydrolysis. The morphology observed in SEM substantiate the idea that loose amorphous regions (Figs. 3a,b) are removed from the entourage of fibers by the hydrolyzing action of PA in (Figs. 3c,d and Supporting Information Fig. S2). These loose moieties then seem to be stabilized within CMC/PA layers which create a thick coating/film on the fibers and around pores. By reacting the foam at 160 °C, cross-linking between all components can then seal the strong fiber-fiber bonds, leading to the observed compressive properties. View of the foam top surfaces clearly shows how the addition of PA induces the formation of a film which closes the pore structure (from Figs. 3e,f to 3g,h). This is likely the reason for the initial reduced moisture uptake in fiber foams reacted with PA during the first 100 h (Supporting Information Fig. S3). Eventually however, all fiber foams maintained a similar moisture uptake compared to the blank foams (7 (*w/w*)% water uptake at 75 % RH). This result was unexpected when considering the significant increase in potential hydrogen bond terminals introduced with PA phosphates. This suggests that the outcome of the cross-linking reactions between cellulose and PA, at the concentrations proposed in this work, does not significantly increase their water vapor intake capacity.

3.3. Fire-retardant behaviour of solid foams

The mechanisms which govern the ability of phytic acid (PA) to create a fire-protective char layer are well described in literature (Horrocks & Price, 2001). The first shoulder in TGA upon increasing temperature represents the onset of carbonization (T_{onset} in Fig. 4a). Here, phosphoric acids lower the carbonization onset temperature by catalyzing the dehydration of cellulose to form a protective char layer against heat and oxygen. The formation of the char layer is marked by significant weight loss between 250 and 350 °C as thermal decomposition creates char and volatiles.

Cellulose fiber foams reacted with phytic acid (PA) presented carbonization onset temperatures reduced by 15 °C, leading to a 20 % higher carbonization rate and reduced weight loss by 10 % compared to foams reacted with CA or no acids (Fig. 4b, c and d, respectively). When applying higher reaction temperatures, the onset, weight loss and carbonization rate increased. An increased onset temperature may signify the formation of ester bonds when phosphorylating cellulose, blocking the depolymerization of cellulose into volatile monomers during carbonization (Ghanadpour et al., 2015). It is also suggested that the thermal decomposition of PA at 160 °C may form volatile phosphoric acids, reducing the potential for catalytic dehydration (Daneluti & Matos, 2013). As a result of this, the char layer barrier may be less efficient at preventing material loss during its formation, and may be thinner from the reduced phosphorus content. At higher PA concentrations as used in other studies, the relative difference in carbonization onset temperatures was higher than observed in this study (Barbalini et al., 2019; Cheng et al., 2022; Feng et al., 2017; Ghanadpour et al., 2015; Jiang et al., 2012;Ma et al., 2021; Sun et al., 2021). The presence of a char barrier increased thermo-oxidative stability in the temperature range of 350–500 °C, reducing the material degradation rates and resulting in a 0.6 % increase in residual mass (Supporting Information Table S2). Addition of PA also raised the combustion temperature (T_{max2}) of cellulose fiber foams from 427 to 498 °C (Fig. 4a and Supporting Information Table S2). This phenomena was not observed with cellulose papers (Orzan et al., 2024). We ascribe the observed difference to the strong interaction between PA and CMC which prevents early thermal degradation of CMC (380 °C) (El-Sayed, Mahmoud, Fatah, & Hassen, 2011; Mostafa, Ali, El-Wassefy, Saad, & Hussein, 2024). Some

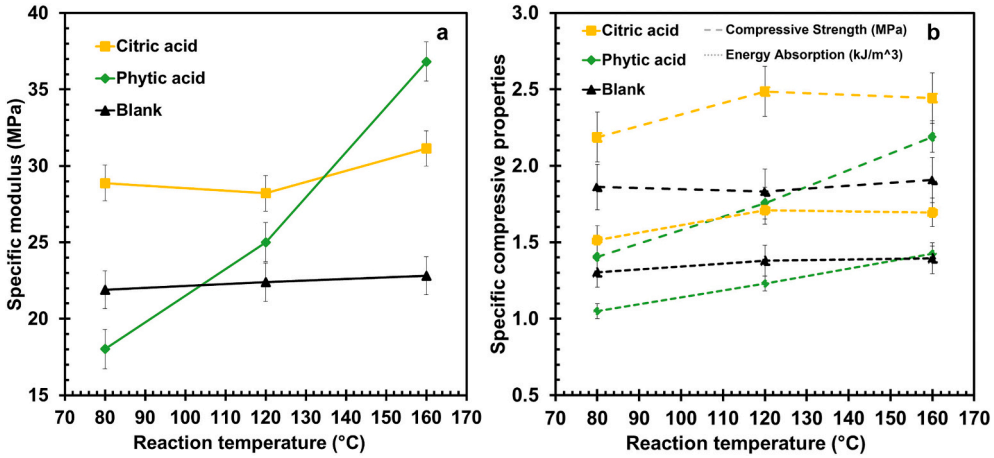

Fig. 2. Compressive properties of solid foams reacted at 80, 120 and 160 °C with either PA, CA, or no acid added. The a) specific modulus represents the stiffness of the solid foams while b) strength and energy absorption represent how much load the solid foams can withstand at higher strains.

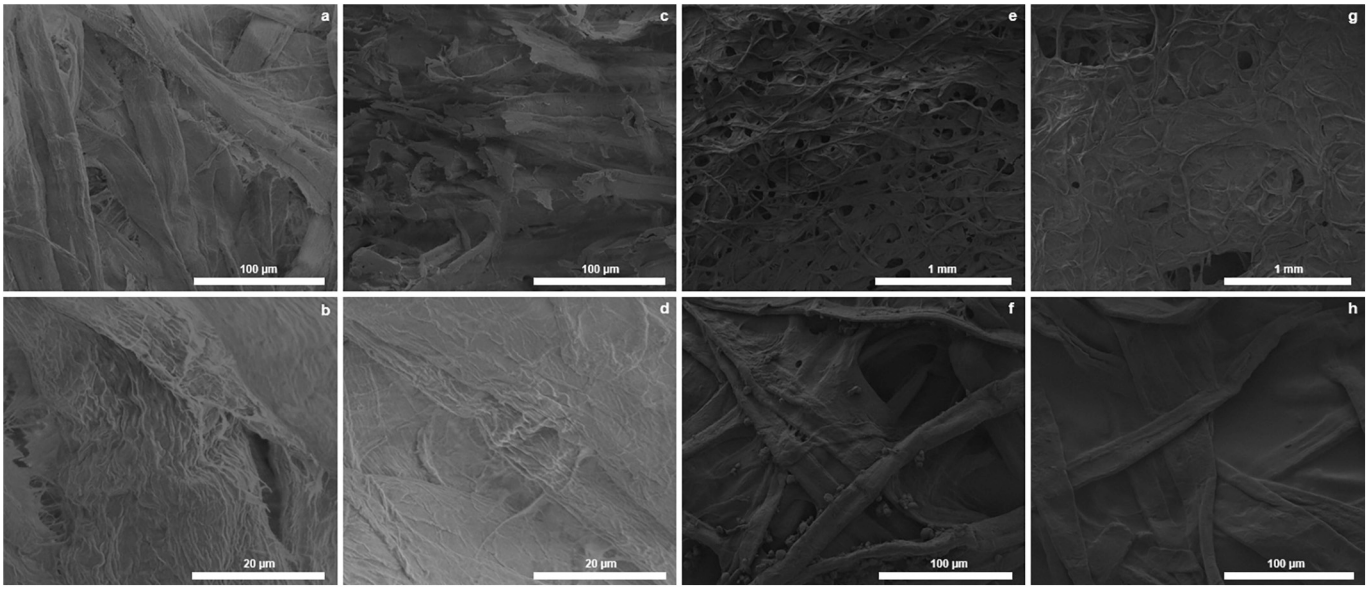

Fig. 3. SEM imaging of cellulose fiber foams with particular magnifications of a) inside blank (160) x1000, b) inside blank (160) x5000, c) inside P160 x1000, d) inside P160 x5000, e) top surface blank (160) x100, f) top surface blank (160) x1000, g) top surface P160 x100, h) top surface P160 x1000.

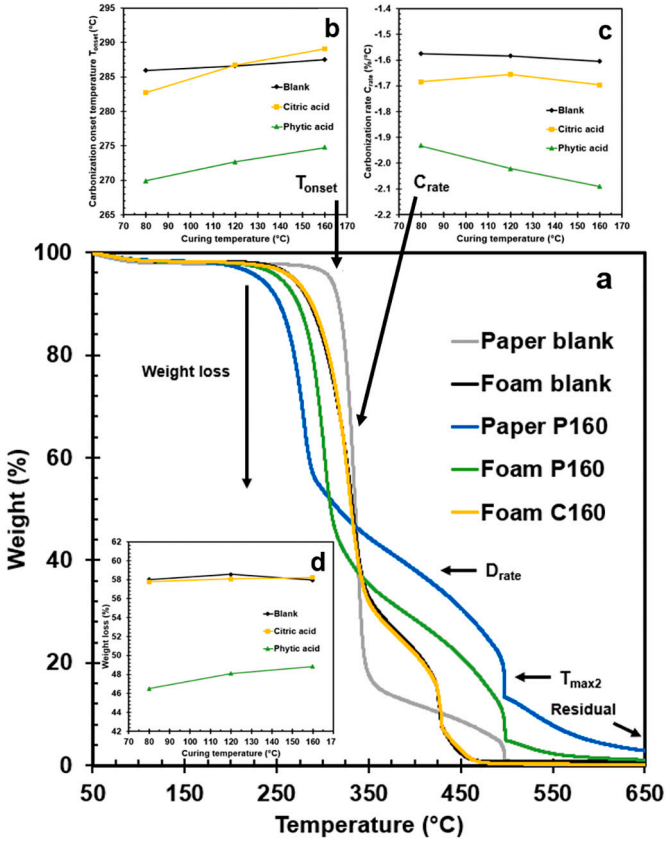

Fig. 4. Thermogravimetric analysis (TGA) results in air for a) overall curves of foam samples with analyzed parameters compared to filter paper results. (Orzan et al., 2024) Effect of reaction temperature was determined via differences in b) carbonization onset temperature (T_{onset} (°C)) at 90 % weight, c) carbonization rate (C_{rate} (%/°C)) at maximum slope, d) weight loss (%) between T_{onset} and plateau. Tabulated values can be found in Supporting Information Table S2.

studies observe differences in the onset temperature (Barbalini et al., 2019; Ghanadpour et al., 2015; Sun et al., 2021), while others found no difference (Ma et al., 2021; Sun et al., 2021).

Cellulose fiber foams reacted with CA performed similarly to blank foams, yet developed a reduced carbonization onset for C80 and an increase in residual weight. The difference in onset suggests that cross-linking delays the initial degradation of cellulose on the surface by forming a non-volatile aliphatic layer, which remains stable after combustion. Furthermore, cone calorimetry results for foam with CA were poor when evaluating time to ignition (TTI), total heat release (THR) and total smoke production (TSP) (Table 2 and Supporting Information Fig. S4). An increased TTI and time to peak heat release rate (TP) suggest that CA delays the onset of material flammability. The increased time to reach PHRR lead to a lower fire growth rate (FGR) with higher cross-linking degree. However, given the high values of PHRR, THR and TSP for CA foams compared to the blank ones, the fire-retardant performance when burning was not improved even when cross-linked.

Cross-linking PA at reaction temperatures above 120 °C caused TTI values to decrease by 43 % for P120 and 60 % for P160. PHRR also decreased by 28 % compared to blank foams. Notably, this decrease correlated with findings by Cheng et al. (2022), who employed a dicyandiamide crosslinker and reported twice the phosphorus content found in our work. The FGR for both P120 and P160 decreased by 53 % from blank foams and smoke production (TSP) was reduced by 64 %.

Table 2
Cone calorimetry analysis of cellulose fiber foams reacted with phytic acid (P), citric acid (C) or no acid at temperatures of 80, 120 and 160 °C. Parameters are defined as follows: time to ignition (TTI), peak heat release rate (PHRR), time to PHRR (TP), total heat release (THR), fire growth rate (FGR), total smoke production (TSP), and smoke production rate (SPR).

Foam	TTI (s)	PHRR (kW/m^2)	TP (s)	FGR (kJ/m^2/s)	THR (MJ/m^2)	TSP (m^2)
80	9.3	118	13	9.1	20	0.11
120	9.3	117	13	9.0	20	0.23
160	4.7	119	13	9.2	18	0.14
P80	8.3	99	13	7.6	19	0.03
P120	4.7	85	21	4.0	18	0.06
P160	3.3	86	19	4.5	17	0.05
C80	9.7	133	16	8.3	22	0.13
C120	9.7	124	18	6.9	22	0.22
C160	8.3	116	21	5.5	21	0.19

Sun et al. (2021) reported similar TTI and TP, yet the phosphorus content was five times higher and the TSP/SPR values were significantly higher. Several other studies employed excessive ratios of phosphorus to cellulose which expectedly resulted in significantly improved properties (Antoun et al., 2022; Ma et al., 2021). In the context of material flame-retardancy performance, the foams presented in this work can be classified as self-extinguishing yet not non-flammable (Antoun et al., 2022).

4. Conclusion

Phytic acid has found a new dimension of applicability: within cellulose-based foams. In wet foam systems, phytic acid had little effect on the foaming behaviour of SDS, yet reacted synergistically with CMC to form homogeneous wet foams with high foamability. The acidic nature of phytic acid caused CMC and SDS to protonate in solutions without a buffer, reducing electrostatic repulsion between bubbles. The resulting wet foams were susceptible to coalescence, causing them to collapse rapidly after mixing. However, this collapse was avoided by drying the wet foams into solid foams directly after foaming. The dried cellulose fiber foams were reacted at temperatures of 80, 120 and 160 °C to evaluate the effect of cross-linking with phytic acid on compressive and fire-retardant performance. The degradation experienced by cellulose fibers from exposure to phytic acid negatively affected the compressive properties of solid foams reacted at 80 and 120 °C. At 160 °C, however, the compressive strength and stiffness of cellulose fiber solid foams increased significantly as cross-links between phytic acid and cellulose reinforced the fiber network. Imaging revealed the formation of a film coating fibers with the addition of PA, which solidified fiber-fiber bonding under cross-linking. Furthermore, the phytic acid foams successfully formed a self-extinguishing char layer and presented significant decreases in heat release rate, fire growth rate, and smoke production compared to fiber foams with and without citric acid.

The era of finding bio-based solutions to engineering problems has come to a turning point; finding practical applications for exciting new compounds is now paramount. In this study, we demonstrate how phytic acid can be a solution toward the creation of strong, fire-retardant cellulose fiber foams. The efficient cross-linking methodology and sparing use of phytic acid presented here provides true scale-up viability for these materials.

CRediT authorship contribution statement

E. Orzan: Writing – review & editing, Writing – original draft, Methodology, Investigation, Formal analysis, Data curation, Conceptualization. **A. Barrio:** Writing – review & editing, Methodology, Investigation, Formal analysis, Conceptualization. **V. Biegler:** Writing – review & editing, Methodology, Investigation. **J.B. Schaubeder:** Writing – review & editing, Investigation. **A. Bismarck:** Writing – review & editing, Supervision, Conceptualization. **S. Spirk:** Writing – review & editing, Supervision, Data curation, Conceptualization. **T. Nypelö:** Writing – review & editing, Supervision, Investigation, Funding acquisition, Conceptualization.

Declaration of competing interest

The authors declare that they have no known competing financial interests or personal relationships that could have appeared to influence the work reported in this paper.

Data availability

Data will be made available on request.

Acknowledgements

The authors would like to thank Florian Feist, Georg Baumann and Markus Wagner from the Vehicle Safety Institute at Graz University of Technology for sharing their expertise regarding compressive testing. Thank you to Nina Kann for the guidance and support regarding analysis of phosphorus compounds. This work has received funding from the European Union's Horizon 2020 - Research and Innovation Framework Programme under grant agreement No 964430. Tiina Nypelö acknowledges the funding from Wallenberg Wood Science Center and Area of Advance Materials, Chalmers University of Technology.

Appendix A. Supplementary data

Supplementary data to this article can be found online at https://doi.org/10.1016/j.carbpol.2024.122617.

References

Antoun, K., Ayadi, M., El Hage, R., Nakhl, M., Sonnier, R., Gardiennet, C., Le Moigne, N., Besserer, A., & Brosse, N. (2022). Renewable phosphorous-based flame retardant for lignocellulosic fibers. *Industrial Crops and Products, 186*, Article 115265.

Barbalini, M., Bertolla, L., Toušek, J., & Malucelli, G. (2019). Hybrid silica-phytic acid coatings: Effect on the thermal stability and flame retardancy of cotton. *Polymers, 11*, 1664.

Bikerman, J. J. (1973). *Foams*. New York: Springer-Verlag.

Cai, X., Chen, H., Wang, Z., Sun, W., Shi, L., Zhao, H., & Lan, M. (2019). 3d graphene-based foam induced by phytic acid: An effective enzyme-mimic catalyst for electrochemical detection of cell-released superoxide anion. *Biosensors and Bioelectronics, 123*, 101–107.

Cheng, X.-W., Wang, Z.-Y., Jin, W.-J., & Guan, J.-P. (2022). Covalent flame-retardant functionalization of wool fabric using ammonium phytate with improved washing durability. *Industrial Crops and Products, 187*, Article 115332.

Daneluti, A. L. M., & Matos, J.d. R. (2013). Study of thermal behavior of phytic acid, Brazilian. *Journal of Pharmaceutical Sciences, 49*, 275–283.

Demitri, C., Del Sole, R., Scalera, F., Sannino, A., Vasapollo, G., Maffezzoli, A., Ambrosio, L., & Nicolais, L. (2008). Novel superabsorbent cellulose-based hydrogels crosslinked with citric acid. *Journal of Applied Polymer Science, 110*, 2453–2460.

Ding, H., Qiu, S., Wang, X., Song, L., & Hu, Y. (2021). Highly flame retardant, low thermally conducting, and hydrophobic phytic acid-guanazole-cellulose nanofiber composite foams. *Cellulose, 28*, 9769–9783.

Du, P., Zhang, J., Guo, Z., Wang, H., Luo, Z., Fan, Z., Li, B., Cai, Z., & Ge, F. (2022). A novel breathable flexible metallized fabric for wearable heating device with flame-retardant and antibacterial properties. *Journal of Materials Science and Technology, 122*, 200–210.

El-Sayed, S., Mahmoud, K., Fatah, A., & Hassen, A. (2011). Dsc, tga and dielectric properties of carboxymethyl cellulose/polyvinyl alcohol blends. *Physica B: Condensed Matter, 406*, 4068–4076.

Evans, D. F., & Wennerström, H. (1999). *The colloidal domain: Where physics, chemistry, biology, and technology meet*. New York: Wiley-Vch.

Feng, Y., Zhou, Y., Li, D., He, S., Zhang, F., & Zhang, G. (2017). A plant-based reactive ammonium phytate for use as a flame-retardant for cotton fabric. *Carbohydrate Polymers, 175*, 636–644.

Ferreira, E. S., Cranston, E. D., & Rezende, C. A. (2020). Naturally hydrophobic foams from lignocellulosic fibers prepared by oven-drying. *ACS Sustainable Chemistry & Engineering, 8*, 8267–8278.

Ferreira, E. S., Rezende, C. A., & Cranston, E. D. (2021). Fundamentals of cellulose lightweight materials: Bio-based assemblies with tailored properties. *Green Chemistry, 23*, 3542–3568.

Frone, A. N., Panaitescu, D. M., Nicolae, C. A., Gabor, A. R., Trusca, R., Casarica, A., … Salageanu, A. (2020). Bacterial cellulose sponges obtained with green cross-linkers for tissue engineering. *Materials Science and Engineering: C, 110*, Article 110740.

Ganesan, K., Barowski, A., Ratke, L., & Milow, B. (2019). Influence of hierarchical porous structures on the mechanical properties of cellulose aerogels. *Journal of Sol-Gel Science and Technology, 89*, 156–165.

Gao, T., Wu, S., Li, X., Lin, C., Yue, Q., Tang, X., … Xiao, D. (2022). Phytic acid assisted ultra-fast in situ construction of ni foam-supported amorphous ni–fe phytates to enhance catalytic performance for the oxygen evolution reaction, inorganic chemistry. *Frontiers, 9*, 3598–3608.

Ghanadpour, M., Carosio, F., Larsson, P. T., & Wågberg, L. (2015). Phosphorylated cellulose nanofibrils: A renewable nanomaterial for the preparation of intrinsically flame-retardant materials. *Biomacromolecules, 16*, 3399–3410.

Ghilan, A., Nita, L. E., Pamfil, D., Simionescu, N., Tudorachi, N., Rusu, D., , … Ciolacu, D. E., et al. (2022). One-step preparation of carboxymethyl cellulose—Phytic acid hydrogels with potential for biomedical applications. *Gels, 8*, 647.

Gibson, L. J. (2003). Cellular solids. *MRS Bulletin, 28*, 270–274.

Guerrini, M. M., Lochhead, R. Y., & Daly, W. H. (1999). Interactions of aminoalkylcarbamoyl cellulose derivatives and sodium dodecyl sulfate. 2. Foam stabilization. *Colloids and Surfaces A: Physicochemical and Engineering Aspects, 147*, 67–78.

Hassan, M. M., Tucker, N., & Le Guen, M. J. (2020). Thermal, mechanical and viscoelastic properties of citric acid-crosslinked starch/cellulose composite foams. *Carbohydrate Polymers, 230*, Article 115675.

Horrocks, A. R., & Price, D. (2001). *Fire retardant materials*. Woodhead Publishing.
Hou, F., Zhu, M., Liu, Y., Zhu, K., Xu, J., Jiang, Z., Wang, C., & Wang, H. (2022). A self-assembled bio-based coating with phytic acid and dl-arginine used for a flame-retardant and antibacterial cellulose fabric. *Progress in Organic Coatings, 173*, Article 107179.
Jiang, G., Qiao, J., & Hong, F. (2012). Application of phosphoric acid and phytic acid-doped bacterial cellulose as novel proton-conducting membranes to pemfc. *International Journal of Hydrogen Energy, 37*, 9182–9192.
Ketoja, J. A., Paunonen, S., Jetsu, P., & Pääkkönen, E. (2019). Compression strength mechanisms of low-density fibrous materials. *Materials, 12*, 384.
Li, X., Sun, H., He, R., Liu, Y., & Wang, Q. (2023). Biomass-based coating for paper fabric with excellent flame retardancy for improved durability humidity/pressure sensors. *Chemical Engineering Journal, 458*, Article 141535.
Liu, J., Qi, P., Meng, D., Li, L., Sun, J., Li, H., Gu, X., Jiang, S., & Zhang, S. (2022). Eco-friendly flame retardant and smoke suppression coating containing boron compounds and phytic acids for nylon/cotton blend fabrics. *Industrial Crops and Products, 186*, Article 115239.
Liu, X.-H., Zhang, Q.-Y., Cheng, B.-W., Ren, Y.-L., Zhang, Y.-G., & Ding, C. (2018). Durable flame retardant cellulosic fibers modified with novel, facile and efficient phytic acid-based finishing agent. *Cellulose, 25*, 799–811.
Ma, Y., Luo, X., Liu, L., Zhang, C., Shang, X., & Yao, J. (2021). Eco-friendly, efficient and durable fireproof cotton fabric prepared by a feasible phytic acid grafting route. *Cellulose, 28*, 3887–3899.
Meftahi, A., Khajavi, R., Rashidi, A., Rahimi, M., & Bahador, A. (2018). Preventing the collapse of 3d bacterial cellulose network via citric acid. *Journal of Nanostructure in Chemistry, 8*, 311–320.
Moosavi-Movahedi, A., Gharanfoli, M., Nazari, K., Shamsipur, M., Chamani, J., Hemmateenejad, B., Alavi, M., Shokrollahi, A., Habibi-Rezaei, M., Sorenson, C., et al. (2005). A distinct intermediate of rnase a is induced by sodium dodecyl sulfate at its pka. *Colloids and Surfaces B: Biointerfaces, 43*, 150–157.
Mostafa, S. I., Ali, M. A., El-Wassefy, N. A., Saad, E. M., & Hussein, M. H. (2024). Adsorption and interaction studies of methylene blue dye onto agar-carboxymethylcellulose-silver nanocomposite in aqueous media. *Biomass Conversion and Biorefinery, 14*, 3363–3383.
Orzan, E., Barrio, A., Spirk, S., & Nypelö, T. (2024). Elucidation of cellulose phosphorylation with phytic acid. *Industrial Crops and Products, 218*.
Pöhler, T., Ketoja, J. A., Lappalainen, T., Luukkainen, V.-M., Nurminen, I., Lahtinen, P., & Torvinen, K. (2020). On the strength improvement of lightweight fibre networks by polymers, fibrils and fines. *Cellulose, 27*, 6961–6976.
Ren, X., Song, M., Jiang, J., Yu, Z., Zhang, Y., Zhu, Y., Liu, X., Li, C., Oguzlu-Baldelli, H., & Jiang, F. (2022). Fire-retardant and thermal-insulating cellulose nanofibril aerogel modified by in situ supramolecular assembly of melamine and phytic acid. *Advanced Engineering Materials, 24*, 2101534.
Song, F., Zhao, Q., Zhu, T., Bo, C., Zhang, M., Hu, L., Zhu, X., Jia, P., & Zhou, Y. (2022). Biobased coating derived from fish scale protein and phytic acid for flame-retardant cotton fabrics. *Materials & Design, 221*, Article 110925.
Štiglic, A. D., Gürer, F., Lackner, F., Bračič, D., Winter, A., Gradišnik, L., , … Plavec, J., et al. (2022). Organic acid cross-linked 3d printed cellulose nanocomposite bioscaffolds with controlled porosity, mechanical strength, and biocompatibility. *IScience, 25*.
Sun, L., Wang, H., Li, W., Zhang, J., Zhang, Z., Lu, Z., … Dong, C. (2021). Preparation, characterization and testing of flame retardant cotton cellulose material: Flame retardancy, thermal stability and flame-retardant mechanism. *Cellulose, 28*, 3789–3805.
Theander, O., & Westerlund, E. A. (1986). Studies on dietary fiber. 3. Improved procedures for analysis of dietary fiber. *Journal of Agricultural and Food Chemistry, 34*, 330–336.
Thota, S., Somisetti, V., Kulkarni, S., Kumar, J., Nagarajan, R., & Mosurkal, R. (2020). Covalent functionalization of cellulose in cotton and a nylon-cotton blend with phytic acid for flame retardant properties. *Cellulose, 27*, 11–24.
Xiao, Y., Gong, X., & Zhang, J. (2021). Self-foaming metal-organic gels based on phytic acid and their mechanical, moldable, and load-bearing properties., chemistry–a. *European Journal, 27*, 8791–8798.
Yang, C. Q., Wang, X., & Kang, I.-S. (1997). Ester crosslinking of cotton fabric by polymeric carboxylic acids and citric acid. *Textile Research Journal, 67*, 334–342.
Zheng, X.-T., Dong, Y.-Q., Liu, X.-D., Xu, Y.-L., & Jian, R.-K. (2022). Fully bio-based flame-retardant cotton fabrics via layer-by-layer self assembly of laccase and phytic acid. *Journal of Cleaner Production, 350*, Article 131525.
Zhivkov, A. M. (2013). Electric properties of carboxymethyl cellulose. In T. van de Ven, & L. Godbout (Eds.), *Cellulose–Fundamental Aspects*. Rijeka, Croatia: IntechOpen.